SCIENTIFIC RESEARCH

VALUE OF DUAL-ENERGY COMPUTED TOMOGRAPHY IN THE ASSESSMENT OF PRIMARY LUNG CANCER

Do Dang Khanh, Nguyen Van Thi**, Doan Van Hoan*, Dinh Hoang Viet**, Ngo Le Lam**, Cao Van Chinh***, Ngo Xuan Thang*, Nguyen Thai Hung**

SUMMARY

Objective: This study aims to observe the value of the dual-energy computed tomography (DECT) technique in the assessment of primary lung cancer. Compare the difference in density of lung tumors on the true non-contrast (TNC) and virtual non-contrast (VNC) images. Investigate the iodine concentration value of lung tumors in differentiating malignant and benign lesions as well as adenocarcinoma and squamous carcinoma in lung cancer.

Methods: We conducted a cross-sectional descriptive study in 42 patients with solitary pulmonary nodules proved by pathology underwent double-phase enhanced CT scan at the Diagnostic Imaging Center of K Hospital, Hanoi. Process dual-energy CT data into virtual monoenergetic and virtual non-contrast images, comparing with true non-contrast images. Compare the iodine concentration of malignant and benign lesions, adenocarcinoma, and squamous cell carcinoma lung cancer. The slope rate was calculated from the spectral curve. Patients were divided into an inflammatory group, a malignant group, and a tuberculosis group. The Kruskal–Wallis test and Nemenyi test were performed to compare quantitative parameters among the three groups.

Results: The study comprised 42 patients (34 males). The mean age of patients was 56 ±11. 23/42 right lung tumors (accounted for about 55%), 13/33 left lung tumors (about 40%). Pathological results showed that 73.8% (31/42) of the lesions were malignant, and 26.2% were benign. The density of lung tumors on the true non-contrast (TNC) and virtual non-contrast (VNC) images is 43,81 ± 10,90 and 43,32 ± 11,15 HU (p=0,147). The contrast-noise ratio of lung tumors has the highest value in the virtual monochrome image at 65 keV. The iodine concentration of malignant tumors was 0,37±0,15mg/ml, higher than benign lesions. The normalized iodine concentration (nIC) of lung tumors can differentiate malignant from benign lesions with an area under the curve of 0,748, with a best cut-off point of 0,27 mg/ml having a sensitivity is 74,2%, specificity of 81,8%. The normalized iodine concentration (nIC) of lung tumors can also differentiate adenocarcinoma from squamous cell carcinoma with an area under the curve of 0,835, with a best cut-off point of 0,36 mg/ml having a sensitivity is 76,5%, specificity of 100%. The mean slope rate for

** Hanoi Medical University*

*** K hospital*

**** Hanoi Medical College*

the inflammatory group was 2,51 ± 0,25, significantly higher than these parameters for the malignant group ($p < 0.05$), and the parameters for the malignant group were significantly higher than the tuberculosis group ($p < 0.05$).

Conclusion: Virtual non-contrast images can replace the role of true non-contrast images. In virtual monoenergetic, the 65 keV sequence has the best Contrast to Noise Ratio (CNR). Quantitative analysis of iodine concentration in lung tumors can help differentiate malignant and benign lung lesions, adenocarcinoma, and squamous cell carcinoma. HU slope rate showed statistically significant differences, which is helpful in the differential diagnosis among inflammatory, malignant, and tuberculosis lesions.

Keywords: *primary lung cancer, DECT, virtual non-contrast images, iodine concentration, virtual monochromatic.*

I. INTRODUCTION

Lung cancer is one of the most common cancers in the world. According to GLOBOCAN 2020, lung cancer ranks second among the most common cancers in the world as well as Vietnam. Lung cancer is also one of the leading causes of death among cancers [1]. Despite progress, many challenges remain in determining the effectiveness of lung cancer diagnosis and treatment.

Many imaging techniques have been used to detect, diagnose, and follow lung cancer, but computed tomography (CT) is still the main method because it provides high-resolution anatomical images. Recently, the most stage-of-the-art CT techniques allowed the use of contrast agents to evaluate vascular proliferation and other imaging features of the tumor. In particular, the dual-energy CT (DECT) technique is based on a dual-source CT system or a fast kV-switching DECT system, taking advantage of the material decomposition theory, while providing virtual non-contrast images and Iodine maps from a single contrast injection [2]. In Vietnam, there are still only a few studies on the application of data obtained from dual-energy CT in lung cancer assessment. Therefore, we conducted this study to evaluate the value of dual-energy CT in diagnosing primary lung cancer and differentiating between benign and malignant lesions as well as some subtypes of lung cancer.

II. METHODS

Subjects

42 patients with lesions suspected of lung cancer underwent dual-energy CT scans at K Hospital Diagnostic Imaging Center, Hanoi from March 2022 to February 2023 and were pathologically confirmed from the core-needle biopsy and/or post-operative specimens.

Methods

The study was conducted using a cross-sectional descriptive method, collecting retrospective and prospective data with convenient model selection. Patients who meet the criteria: have lesions suspected of lung cancer, have dual-energy CT scan with proper technique, and have pathology results from core-needle biopsy specimens and/or after surgery. The patients were taken by a Revolution HD (GE) 128-slide dual-energy CT scanner at K Hospital Diagnostic Imaging Center, Hanoi. Process images using GSI Volume Viewer software (AW 4.7). Use Iodine dehydration imaging to analyze Iodine-based materials, measuring HU parameters and Iodine concentration (using quantitative analysis). We set ROI to measure the Iodine concentration parameter in the lesion (IC: mg/ml) during the venous phase: measure the largest diameter of the lesion on the Axial plane. Place the ROI in the position with the highest contrast enhancement and copy it to the normal parenchyma.

Place the ROI on the aorta and calculate the nIC value according to the formula $nIC=IC/IC_{aorta}$ (with IC_{aorta} as the iodine concentration measured in the thoracic aorta during the same venous phase).

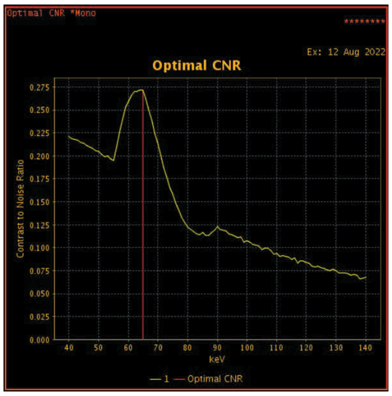

Figure 1. Iodine CNR of virtual monochromatic CT images at energies ranging from 40 keV to 140 keV.

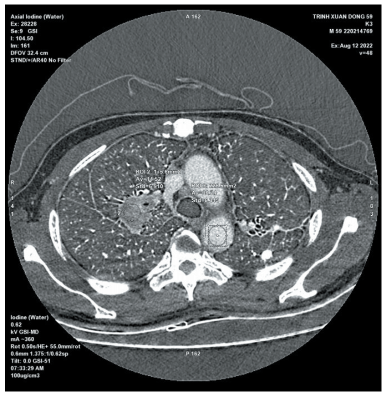

Figure 2. Example image of IC measurements: ROI in thoracic aorta and lesion.

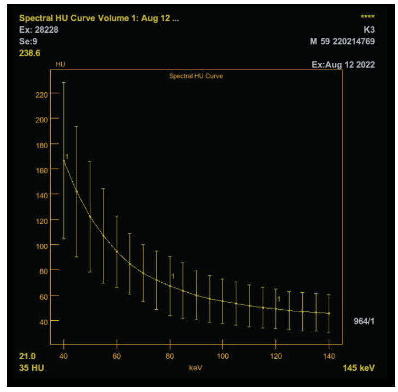

Figure 3. Construct spectral HU Curve ranging from 40 keV to 140 keV.

Measuring the density of the lesion on monochromatic images at different energy levels from 40-140 keV, we constructed an HU spectrum curve. Calculate the slope index HU according to the formula with HU_{40keV} being the primary mass density measured at an energy level of 40keV, HU_{100keV} being the primary mass density measured at an energy level of 100keV:

$$\frac{\text{HU40keV} - \text{HU100keV}}{60}$$

Processing and analyzing data

Commercial statistical packages SPSS (version 26.0, Chicago, Ill) were used.

Qualitative variables are described by frequency and percentage. The results were expressed as mean standard ± deviation. The average values are taken to two decimal places and compared pairwise using the T-test if the distribution is normal, and the Wilcoxon non-parametric test if the distribution is skewed. Tests are considered statistically significant when p-value ≤ 0.05. Use Kruskal–Wallis and Nemenyi tests to quantitatively compare HU slopes among 3 groups (inflammation, tuberculosis, and cancer) and each pair of 2 groups.

III. RESULTS

Characteristics of research subjects and lung cancer images with dual-energy CT

42 patients with suspected lung cancer undergoing dual-energy CT scans from March 2022 to February 2023 met the study's selection criteria, including 34 men and 8 women (male: female ratio is 4.25:1). Pathology results included 31 cancer patients and 11 non-cancer patients. The patient group had an average age of 55.6 years, ranging from 22 to 76 years. The average lesion size was 43.3±21.6mm (including 38 solid lesions, 4 part-solid lesions, and 0 ground-glass lesions). The research model shows that lung tumors are located on the right side more than on the left side (accounting for 23/42 patients), of which the largest proportion is in the right upper lobe of the lung, with ratios illustrated in Graph 1.

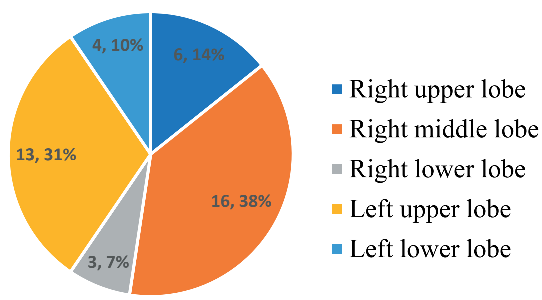

Graph 1. Distribution of lesions

The optimal monochromatic energy level based on calculating the CNR (Contrast to Noise Ratio) is 65 keV.

Table 1. Lesions density in true and virtual non-enhanced images

	True non-enhanced images	Virtual non-enhanced images	p-value
Lesion density (HU)	43,81 ± 10,90	43,32 ± 11,15	0,147

The p-value for comparisons between 2 groups using the T-test.

Lung tumor density between virtual non-enhanced images and true non-enhanced images has no statistically significant difference ($p > 0.05$).

Evaluating the value of dual-energy CT scan in diagnosing lung cancer

The value of IC and nIC indexes in differentiating benign and cancerous lesions

Table 2. Iodine concentration between cancer and non-cancer patients

Iodine concentration parameters	Cancer	Non-cancer	Total	p-value
	n=11	n=31	n=42	
Iodine concentration (IC)	0,99 ± 0,58	1,41 ± 0,58	1,30 ± 0,60	0,05
Normalized iodine concentration (nIC)	0,24 ± 0,15	0,37 ± 0,15	0,34 ± 0,16	0,02

The p-value for comparisons between 2 groups using the T-test.

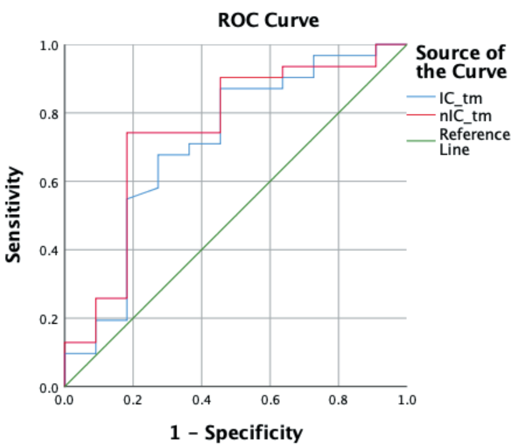

Graph 2. The ROC curves of IC and nIC values for distinguishing between benign and cancerous lesions.

Iodine concentration and normalized Iodine concentrations between the two groups (cancer or non-cancer) had statistically significant differences. According to the study, the area under the curve for venous IC and nIC values were 0.711 and 0.748, respectively. If we take the nIC threshold value of 0.27mg/ml (the cutoff point has the Youden's index = 0.56), we have sensitivity and specificity in diagnosing lesions that are cancerous or non-cancerous, respectively 74.2% and 81.8%.

The value of IC and nIC parameters in differentiating between lung

squamous carcinoma and adenocarcinoma

Table 3. Iodine concentration between lung adenocarcinoma and squamous carcinoma

	Iodine concentration (IC)	Normalized iodine concentration (nIC)
Adenocarcinoma (n=17)	1,60 **± 0,56**	0,41 ± 0,14
Squamous carcinoma (n=5)	1,01 **±** 0.30	0,27 ± 0,06
p-value	0,04	0,04

The p-value for comparisons between 2 groups using the T-test.

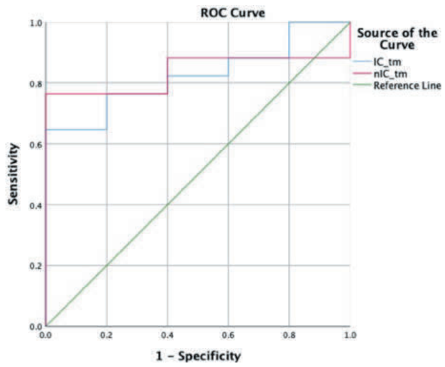

Graph 3. The ROC curves of IC and nIC values for distinguishing between lung squamous carcinoma and adenocarcinoma.

There is a statistically significant difference in the IC and nIC parameters between the adenocarcinoma and squamous carcinoma patient groups. The area under the curve for IC and nIC values were 0.824 and 0.835, respectively. If we take the nIC cutoff point of 0.36mg/ml, the sensitivity and specificity are 76.5% and 100%.

The value of the HU curve in differentiating inflammatory lesions, tuberculosis, and cancer

Table 4. HU slope rate parameter among 3 groups of patients during the venous phase

	Cancer	Inflammatory lesions	Tuberculosis	p
Slope rate (venous phase)	1,73± 0,55	2,51 ± 0,25	0,44 ± 0,07	<0,001 Kruskal–Wallis test

The HU slope rate among patients in the three groups of cancer, inflammation, and tuberculosis is shown in Table 4, which are 1.73±0.55, 2.51±0.25, and 0.44±0, respectively. There was a significant difference between the HU slope rate among the three groups ($p < 0.05$).

Table 5. HU slope rate between each of the 2 groups within the three groups

Groups	p-value
Cancer and inflammatory lesions	0,01
Cancer and tuberculosis	<0,001
Inflammatory lesions and tuberculosis	<0,001

p-value compared among 3 groups by Nemenyi test.

Table 5 compares the HU slope rate between each of the 2 groups in the three groups. It can be seen that the HU slope rate is highest in the inflammation group, followed by the cancer group and the lowest is the tuberculosis group, the difference is significant ($p < 0.05$).

IV. DISCUSSION

The study was conducted on a rapid-switching kVp dual-energy computed tomography scanner (Revolution HD (GE) system). The energy level for optimal monochrome imaging is based on calculating the CNR (Contrast to Noise Ratio) of 65 keV. This is similar to the research of Zegadło et al [3] (suggesting that the optimal energy level is in the range of 40-80 keV) and author Zhang [4] (suggesting that monochrome images are reproduced at an energy level of 65 keV). -75keV reduces noise and increases contrast-to-noise ratio (CNR). The average lung tumor density is 43.81 ± 10.90 and 43.32 ± 11.15 HU in the true non-enhanced images and virtual non-enhanced images, respectively. There was no statistically significant difference, proving that virtual non-enhanced images have tissue density without difference from the true non-enhanced images, this is similar to the study of Le Tan Khiem [5]. This shows that a series of virtual non-enhanced images can replace true non-enhanced images, helping to reduce 55.56% [6] of radiation dose to the patient as well as save CT performing time.

Iodine is a common contrast agent material substance in CT scans. Spectral CT images are particularly sensitive to Iodine so they can accurately and objectively reflect the Iodine concentration parameter through Iodine and water deletion images [7], [8]. An in vivo study compared iodine concentrations via IC spectroscopic imaging with actual in vitro concentrations and reported relative errors of less than 10% [9]. IC is not only closely related to the blood supply of the lesion but is also affected by many different factors such as total dose of contrast agent, flow rate, and blood circulation, or patient factors such as height, weight, and blood pressure. Therefore, the nIC parameter normalized from IC was used in this study. Our results show that the iodine concentration as well as the normalized iodine concentration in the tumor vein have statistically significant differences between cancer patients (n = 31). and non-cancer patients (n=11). This result is similar to the study of Odisio [10] as well as the study of Xiao et al [11] when it was found that the iodine concentration value at the tumor center of cancer lesions was higher than that of benign. Our research results also show that the iodine concentration parameter of adenocarcinoma is higher than that of squamous carcinoma, which is similar to the research of Zhang Z [12] and Le Tan Khiem [5]. This can be explained by some studies that in adenocarcinoma, the microvessel density (MVD) of adenocarcinoma is higher than that of squamous carcinoma. In normal lung parenchyma, endothelial cells are responsible for binding iodine to prevent it from escaping into the interstitial space. When microvascular density is higher in cancerous lung parenchyma due to increased angiogenesis, capillary endothelial cells have loose connections with intact basement membranes, allowing iodine to escape into the interstitial space [13], [14].

The spectral curve is the energy attenuation curve of X-rays when passing through a certain substance. Studies have shown that the spectral curve changes when X-rays pass through tissues with different chemical compositions, so this curve can be used to differentiate tissues [15], [16]. Previous studies have suggested that conventional chest CT and perfusion CT can also differentiate malignant and tuberculosis groups like spectral CT but fail to differentiate malignant nodules and inflammatory lesions. In this study, the HU slope rates of three groups of cancer, inflammation, and tuberculosis were 1.73±0.55, 2.51±0.25 and 0.44±0.07, respectively. During the venous phase, there is a statistically significant difference, this result is quite similar to the study of author Lin et al [17]. The difference in the spectral curves between the three groups can be explained by the different blood supply and the different histological nature of each type of lesion. More specifically, the blood supply of the tumor in lung cancer is mainly from the bronchial artery. The blood vessels are often curved and have an increased diameter, the distance between endothelial cells is widened, contributing to increased vascular permeability. Therefore, tumors will receive blood supply slowly for a long time after contrast injection. Inflammatory lesions are often supplied with blood from both the pulmonary artery and the bronchial artery . Meanwhile, tuberculosis lesions are often poor vascular lesions, so they often have poor enhancement or only enhance the edges. According to some studies, inflammatory lesions often enhance faster and peak faster than cancerous lesions. The lower the energy level, the greater the tissue attenuation value, increasing the difference between the three groups.

V. CONCLUSION

Virtual non-enhanced images can be used to replace the role of true non-enhanced images. Optimal monochrome image quality can be evaluated at the monoenergy level of 65 keV. Quantifying iodine levels can help differentiate between benign and malignant lesions as well as differentiate between adenocarcinoma and squamous carcinoma. The HU slope rate during the venous phase can help differentiate between inflammatory, tuberculosis, and malignant groups.

REFERENCES

1. Sung H, Ferlay J, Siegel RL, et al. Global Cancer Statistics 2020: GLOBOCAN Estimates of Incidence and Mortality Worldwide for 36 Cancers in 185 Countries. *CA Cancer J Clin*. 2021;71(3):209-249. doi:10.3322/caac.21660

2. Zhang LJ, Yang GF, Wu SY, Xu J, Lu GM, Schoepf UJ. Dual-energy CT imaging of thoracic malignancies. *Cancer Imaging*. Published online March 6, 2013:81-91. doi:10.1102/1470-7330.2013.0009

3. A New Outlook on the Ability to Accumulate an Iodine Contrast Agent in Solid Lung Tumors Based on Virtual Monochromatic Images in Dual Energy Computed Tomography (DECT): Analysis in Two Phases of Contrast Enhancement - PMC. Accessed July 9, 2023. https://www.ncbi.nlm.nih.gov/pmc/articles/PMC8123482/

4. Zhang LJ, Wang ZJ, Lu L, Chen B, Lu GM. Feasibility of gadolinium-enhanced dual-energy CT pulmonary angiography: a pilot study in rabbits. *Int J Cardiovasc Imaging*. 2011;27(7):1069-1080. doi:10.1007/s10554-010-9755-4

5. Lê Tấn Khiêm, Nguyễn Thị Minh Trang, Huỳnh Phượng Hải, Lê. Giá trị của chụp cắt lớp vi tính hai mức năng lượng trong đánh giá ung thư phổi. *Tạp Chí Học Tp Hồ Chí Minh*. 2022;Số 26:Tr. 21-27.

6. Nguyễn Mạnh Hùng, Cao Văn Chính, Bùi Văn Giang, Nguyễn Trung Kiên, Đinh Hoàng Việt, Nguyễn Trọng Bang. NGHIÊN CỨU ỨNG DỤNG KỸ THUẬT CHỤP CT HAI MỨC NĂNG LƯỢNG TRONG CHẨN ĐOÁN UNG THƯ PHỔI. *Tạp Chí Học Việt Nam*. 2022;520(2). doi:10.51298/vmj.v520i2.4193

7. Zhang D, Li X, Liu B. Objective characterization of GE discovery CT750 HD scanner: gemstone spectral imaging mode. *Med Phys*. 2011;38(3):1178-1188. doi:10.1118/1.3551999

8. Sudarski S, Apfaltrer P, Nance JW, et al. Optimization of keV-settings in abdominal and lower extremity dual-source dual-energy CT angiography determined with virtual monoenergetic imaging. *Eur J Radiol*. 2013;82(10):e574-581. doi:10.1016/j.ejrad.2013.04.040

9. Lv P, Lin XZ, Li J, Li W, Chen K. Differentiation of small hepatic hemangioma from small hepatocellular carcinoma: recently introduced spectral CT method. *Radiology*. 2011;259(3):720-729. doi:10.1148/radiol.11101425

10. Odisio EG, Truong MT, Duran C, de Groot PM, Godoy MC. Role of Dual-Energy Computed Tomography in Thoracic Oncology. *Radiol Clin North Am*. 2018;56(4):535-548. doi:10.1016/j.rcl.2018.03.011

11. Xiao H, Liu Y, Tan H, et al. A pilot study using low-dose Spectral CT and ASIR (Adaptive Statistical Iterative Reconstruction) algorithm to diagnose solitary pulmonary nodules. *BMC Med Imaging*. 2015;15(1):54. doi:10.1186/s12880-015-0096-6

12. Zhang Z, Zou H, Yuan A, et al. A Single Enhanced Dual-Energy CT Scan May Distinguish Lung Squamous Cell Carcinoma From Adenocarcinoma During the Venous Phase. *Acad Radiol*. 2020;27(5):624-629. doi:10.1016/j.acra.2019.07.018

13. Sikora J, Słodkowska J, Radomyski A, et al. Immunohistochemical evaluation of tumor angiogenesis in adenocarcinoma and squamous cell carcinoma of lung. *Rocz Akad Med W Bialymstoku 1995*. 1997;42 Suppl 1:271-279.

14. Yuan A, Yu CJ, Kuo SH, et al. Vascular endothelial growth factor 189 mRNA isoform expression specifically correlates with tumor angiogenesis, patient survival, and postoperative relapse in non-small-cell lung cancer. *J Clin Oncol Off J Am Soc Clin Oncol*. 2001;19(2):432-441. doi:10.1200/JCO.2001.19.2.432

15. Karçaaltıncaba M, Aktaş A. Dual-energy CT revisited with multidetector CT: a review of principles and clinical applications. *Diagn Interv Radiol Ank Turk*. 2011;17(3):181-194. doi:10.4261/1305-3825.DIR.3860-10.0

16. Deng K, Li W, Wang J jun, Wang G li, Shi H, Zhang C qi. The pilot study of dual-energy CT gemstone spectral imaging on the image quality of hand tendons. *Clin Imaging*. 2013;37(5):930-933. doi:10.1016/j.clinimag.2013.01.008

17. Lin J Zheng, Zhang L, Zhang C yu, Yang L, Lou H Nan, Wang Z Guo. Application of Gemstone Spectral Computed Tomography Imaging in the Characterization of Solitary Pulmonary Nodules: Preliminary Result. *J Comput Assist Tomogr*. 2016;40(6):907-911. doi:10.1097/RCT.0000000000000469

Correspondent: Do Dang Khanh. Email: khanhjhr@gmail.com
Received: 19/09/2023. Assessed: 25/09/2023. Accepted: 23/12/2023